

When Ternary Triangulated Disc Packings Are Densest: Examples, Counter-Examples and Techniques

Thomas Fernique ✉

CNRS & LIPN, Univ. Paris Nord, 93430 Villetaneuse, France

Daria Pchelina ✉ 

LIPN, Univ. Paris Nord, 93430 Villetaneuse, France

Abstract

We consider *ternary* disc packings of the plane, i.e. the packings using discs of three different radii. Packings in which each “hole” is bounded by three pairwise tangent discs are called *triangulated*. Connelly conjectured that when such packings exist, one of them maximizes the proportion of the covered surface: this holds for unary and binary disc packings. For ternary packings, there are 164 pairs (r, s) , $1 > r > s$, allowing triangulated packings by discs of radii 1, r and s . In this paper, we enhance existing methods of dealing with maximal-density packings in order to study ternary triangulated packings. We prove that the conjecture holds for 31 triplets of disc radii and disprove it for 40 other triplets. Finally, we classify the remaining cases where our methods are not applicable. Our approach is based on the ideas present in the Hales’ proof of the Kepler conjecture. Notably, our proof features local density redistribution based on computer search and interval arithmetic.

2012 ACM Subject Classification Theory of computation → Computational geometry

Keywords and phrases Disc packing, density, interval arithmetic

Digital Object Identifier 10.4230/LIPIcs.SoCG.2023.32

Related Version *Full version:* <https://arxiv.org/abs/2211.02905> [17]

Supplementary Material *Software:* https://github.com/tooticki/ternary_triangulated_disc_packings, archived at [swh:1:dir:9630535719e287d4e42724550cdaf81df94181c5](https://swh.1:dir:9630535719e287d4e42724550cdaf81df94181c5)

1 Introduction

Given a finite set S of discs, a *packing* of the plane by S is a collection of translated copies of discs from S with disjoint interiors.

Given a packing P , its *density* $\delta(P)$ is the proportion of the plane covered by the discs. More formally,

$$\delta(P) := \limsup_{n \rightarrow \infty} \frac{\text{area}([-n, n]^2 \cap P)}{\text{area}([-n, n]^2)}.$$

Nowadays, the density of disc packings is widely studied in different contexts. The worst-case optimal density of packings in triangular and circular containers is found in [11, 12]. In computer science, there are various connections between sphere packings and error-correcting codes [4]. Researchers in chemical physics used Monte Carlo simulations on 2-disc packings and, among others, obtained lower bounds on the maximal density of packings with particular disc sizes [7]. Two other groups of physicists found lower bounds on maximal densities of packings in \mathbb{R}^3 with 2 sizes of spheres [26, 31]. Upper bounds on the density are usually much harder to obtain.

The main problem we are interested in is the following: given a finite set of ball sizes in \mathbb{R}^2 (or \mathbb{R}^3), find a packing of the plane (or of the space) maximizing the density.



© Thomas Fernique and Daria Pchelina;

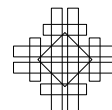
licensed under Creative Commons License CC-BY 4.0

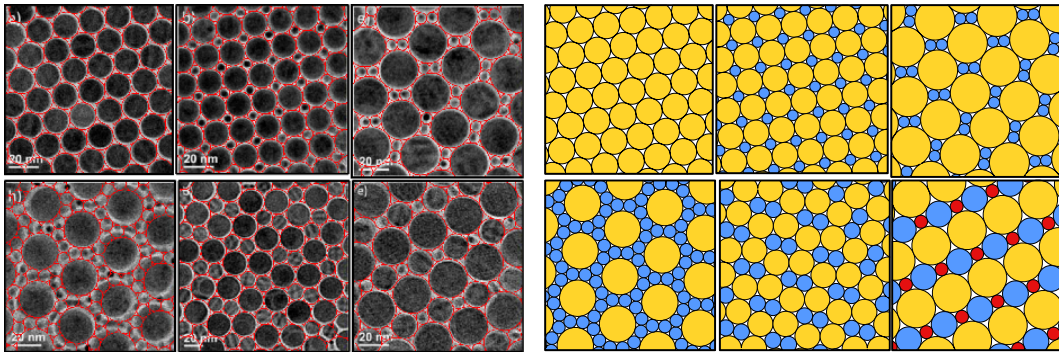
39th International Symposium on Computational Geometry (SoCG 2023).

Editors: Erin W. Chambers and Joachim Gudmundsson; Article No. 32; pp. 32:1–32:17

Leibniz International Proceedings in Informatics

LIPICs Schloss Dagstuhl – Leibniz-Zentrum für Informatik, Dagstuhl Publishing, Germany





■ **Figure 1** Disc packings self-assembled from colloidal nanodiscs and nanorods in [32] (on the left) which very accurately correspond to triangulated packings (on the right).

Answering this question has a few practical applications. Chemists, for example, are interested in the disc and sphere sizes maximizing the density in order to eventually design compact materials using spherical nanoparticles of given sizes [7, 26, 32]. Figure 1 gives an illustration of experimental results from [32].

The first known studies of the densest packings go back to Kepler. Many advances in this area have been made since then.

1.1 1-sphere packings

In a Kepler manuscript dated by 1611, we find a description of the “cannonball” packing followed by an assertion that it is a densest *1-sphere packing* (i.e. packing by equally sized spheres) of the three-dimensional Euclidean space. This assertion is widely known by name of the Kepler conjecture. The “cannonball” packing, also called face-centered-cubic (FCC) packing, belongs to a family of packings formed by stacking layers of spheres centered in the vertices of a triangular lattice, like it is shown in Figure 2. After placing the first two layers, at each step, there are two choices of how to place the next layer. This gives us an uncountable set of packings having the same density. These packings are called *close-packings*.

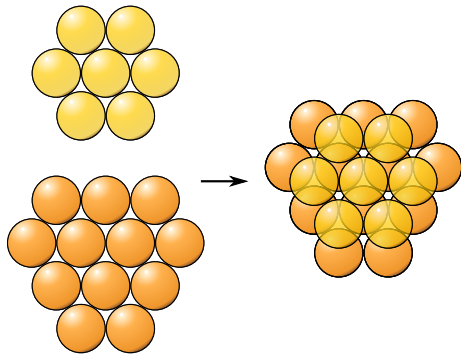
► **Conjecture 1** (Kepler 1611). *The density $\delta(P)$ of packing P of \mathbb{R}^3 by unit spheres never exceeds the density of a close-packing:*

$$\delta(P) \leq \frac{\pi}{3\sqrt{2}}. \quad (1)$$

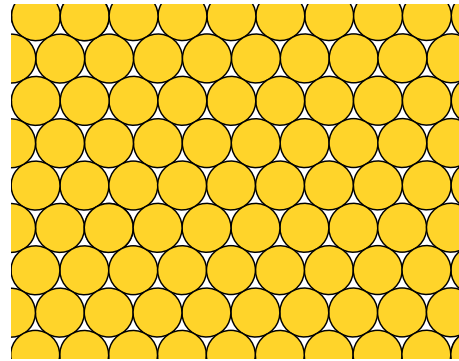
The first advancement in a proof of the Kepler conjecture was made by Gauss who, in 1831, showed that close sphere packings maximize the density among all possible *lattice* packings, i.e. those where the disc centers form a lattice [19]. However, the proof of the whole conjecture took four centuries to be found. Hilbert included this conjecture, also named “the sphere packing problem”, in his famous list of 23 problems published in 1900.

The Kepler conjecture was finally proved in a series of 6 papers submitted by Hales and Ferguson in 1998 [20, 22]. Their computer-assisted proof took 8 years to be fully reviewed. In 2003, Hales founded a project called Flyspeck in order to fully verify his proof by an automated theorem prover. Flyspeck was completed in 2014 including the proof of the Kepler conjecture in the list of computer verified proofs [21].

The rough idea of the proof consists of locally redistributing the density function and showing inequality (1) for this redistributed density. Lagarias calls this approach “localization” [29]. In our work, we use the same general ideas discussed in detail in Section 2.



■ **Figure 2** First step of construction of a 3D close-packing.



■ **Figure 3** 2D hexagonal packing.

1.2 Disc packings

The two-dimensional variant of the Kepler conjecture claims the 2D hexagonal packing on the plane (see Fig. 3) to have the highest density among all planar packings by identical discs.

In 1772, Lagrange proved it to be a densest among lattice packings. The general result was first shown by Thue in 1910 [33]. His proof was however considered incomplete, a reliable proof was given by Fejes-Tóth in 1942 [8].

The proof of the two-dimensional Kepler conjecture contains the basics of the strategy used to prove similar results for packings with several disc sizes, like binary packings (discussed below) and ternary packings which are studied in this paper.

Packings of the plane where, as in the hexagonal one, each “hole” is bounded by three pairwise tangent discs are called *triangulated*. More formally,

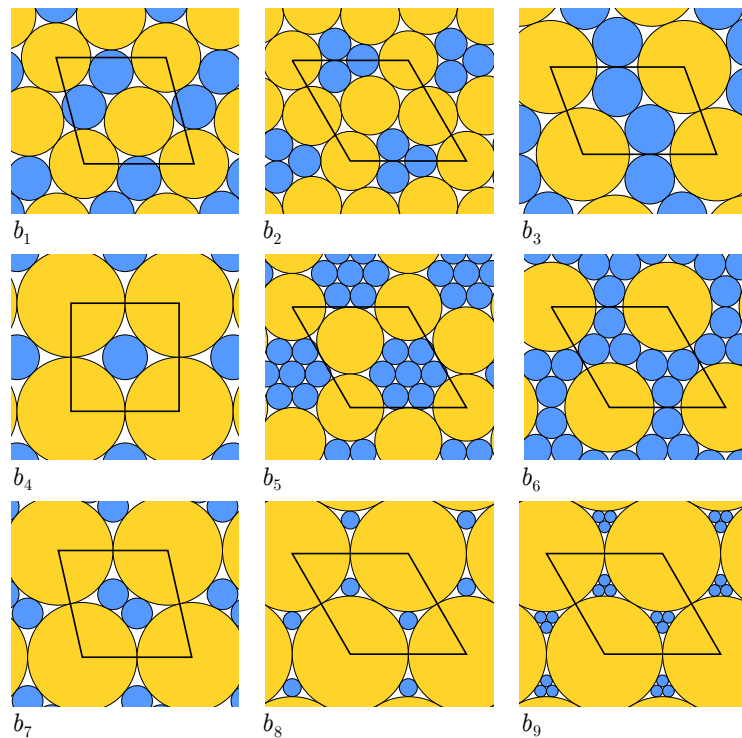
► **Definition 2.** *A packing is called **triangulated** if the graph formed by connecting the centers of every pair of tangent discs is a triangulation.*

Fejes Tóth in [9] called such packings “compact”: since triangulated packings have no “huge holes”, they intuitively look the most compact. Moreover, around each disc, its neighbors form a corona of tangent discs which looks like a locally “optimal” way to pack. For these reasons, triangulated packings appear to be the best candidates to maximize the density on the whole plane.

Notice that, for a fixed n , there exists only a finite number of n -tuples of disc radii (r_1, \dots, r_n) s.t. $1 = r_1 > \dots > r_n > 0$ allowing a triangulated packing where all n disc sizes are present [30].

Let us consider binary packings of the plane. Given two discs of radii 1 and $r < 1$, what is the maximal density of a packing by copies of these discs? We can always obtain $\frac{\pi}{2\sqrt{3}}$, the density of the hexagonal packing, by using only one of the discs which gives as a lower bound on the maximal density. Florian in [18] derived an upper bound on the density which is equal to the density in the triangle formed by 2 small and one big pairwise tangent discs. [14] gives tighter lower and upper bounds of maximal density of binary packings of the plane, for all values of $r \in (0, 1)$.

There are 9 values of r allowing triangulated binary packings where both disc sizes are present [28]. Such packings are shown in Fig. 4. Each of the depicted packings is *periodic*, i.e. if P is a packing in question, there are two non-collinear vectors u and v , called periods, such that $P + u = P + v = P$. Notice that in this paper, we always consider packings of the



■ **Figure 4** 9 triangulated periodic binary packings maximizing the density among packings with the respective disc sizes.

whole plane, and since the triangulated packings we show here and below are all periodic, it is enough to represent their fundamental domain (a parallelogram formed by the period vectors, marked in black in Fig. 4) to see how the whole plane is packed.

Notice that for each of these values of r , there is actually an infinite number of packings having the same density as the one depicted in Fig. 4. First, changing a finite portion of a packings does not affect its density. Moreover, for b_1 , b_3 , and b_7 , there exist non-periodic triangulated packings with a different global structure, having the same density as the ones from Fig. 4 [28]. For the sake of simplicity, we choose to depict the periodic ones.

It turns out that for each of these 9 radii, the density is maximized by a triangulated binary packing – namely, the ones shown in Figure 4 [1, 24, 25, 27]. This result suggests the following conjecture [2].

► **Conjecture 3** (Connelly, 2018). *If a finite set of discs allows a triangulated **saturated** packing, then the density of packings by these discs is maximized on a triangulated packing.*

A packing by a set of discs is called *saturated* if no more discs from this set can be added to the packing without intersecting already placed discs. In our setup, we always assume packings to be saturated since we are interested in the upper bounds on the density.

The Connelly conjecture holds for 1-disc (*unary*) packings and 2-disc (*binary*) packings. To study this conjecture, the next step is to verify it for 3-disc (*ternary*) packings which was the main motivation of our work.

1.3 Our results

Let us turn to the ternary packings. To begin with, we need to find the sizes of discs allowing triangulated ternary packings. This problem was solved in [15]: there are 164 pairs (r, s) featuring triangulated packings with discs of radii $1, r, s$, $1 > r > s$. In this paper, a triplet of disc radii associated to each of such pairs is called a *case*.

The ternary cases are indexed by positive integers from 1 to 164, like in [15]. To avoid confusion, the binary cases (pairs of disc radii allowing binary triangulated packings) are denoted by b_1, \dots, b_9 which respectively correspond to the cases 1–9 in [1].

The Connelly conjecture is applicable only to the cases having triangulated *saturated* packings. This eliminates 15 cases where no triangulated packing is saturated and leaves us with 149 cases.

Our main contribution is a classification of 71 cases formulated in the following theorem:

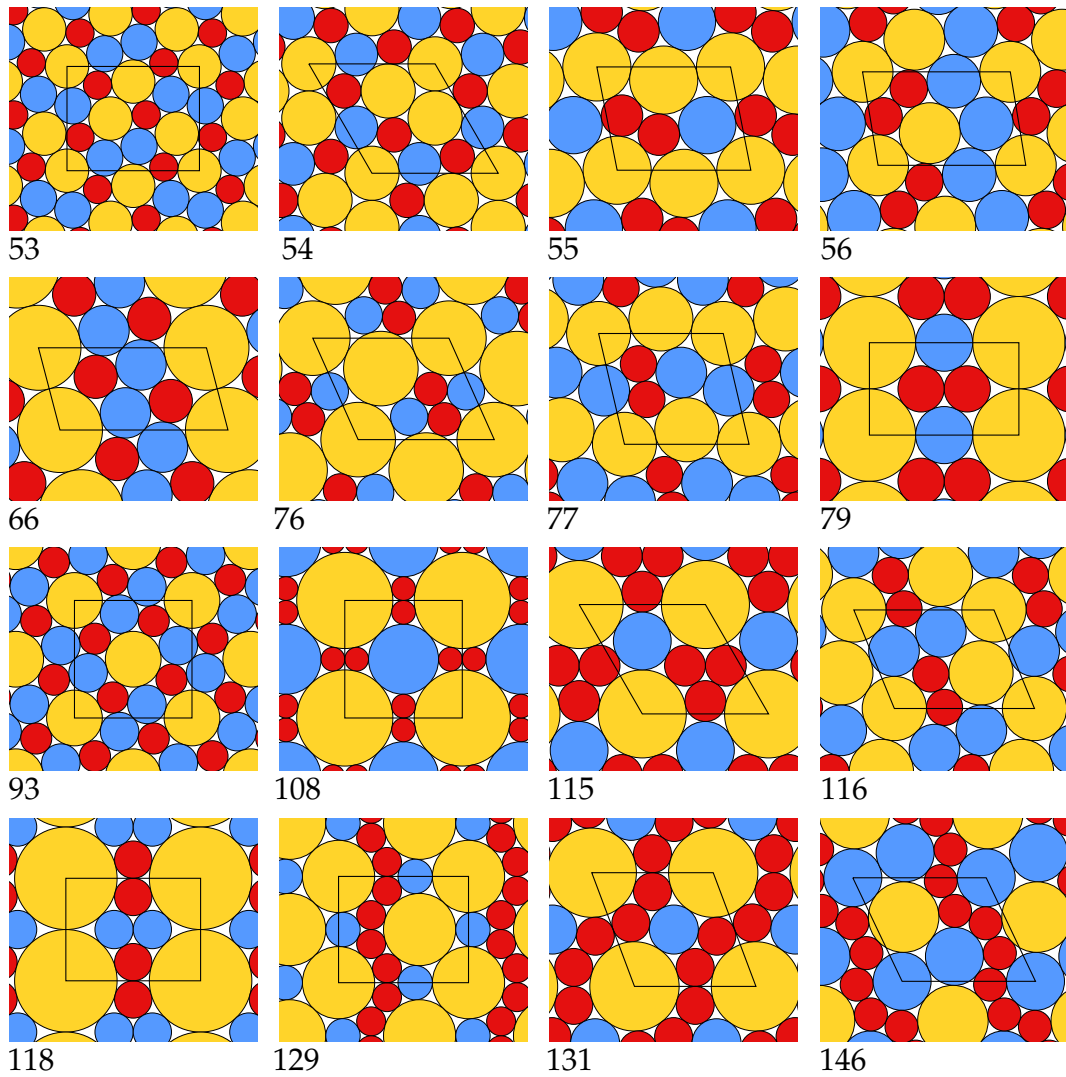
► **Theorem 4.**

- (a) For the 16 following cases: 53, 54, 55, 56, 66, 76, 77, 79, 93, 108, 115, 116, 118, 129, 131, 146, the density is maximized by a triangulated ternary packing.
- (b) For the cases 1–15, the density is maximized by triangulated binary packings. For cases 1–5, it is the triangulated packing of b_8 ; for case 6 – b_4 ; for cases 7–9 – b_7 ; for cases 10–16 – b_9 .
- (c) For the 40 following cases: 19, 20, 25, 47, 51, 60, 63, 64, 70, 73, 80, 92, 95, 97, 98, 99, 100, 104, 110, 111, 117, 119, 126, 132, 133, 135, 136, 137, 138, 139, 141, 142, 151, 152, 154, 159, 161, 162, 163, 164, there exists a non-triangulated packing denser than any triangulated one.

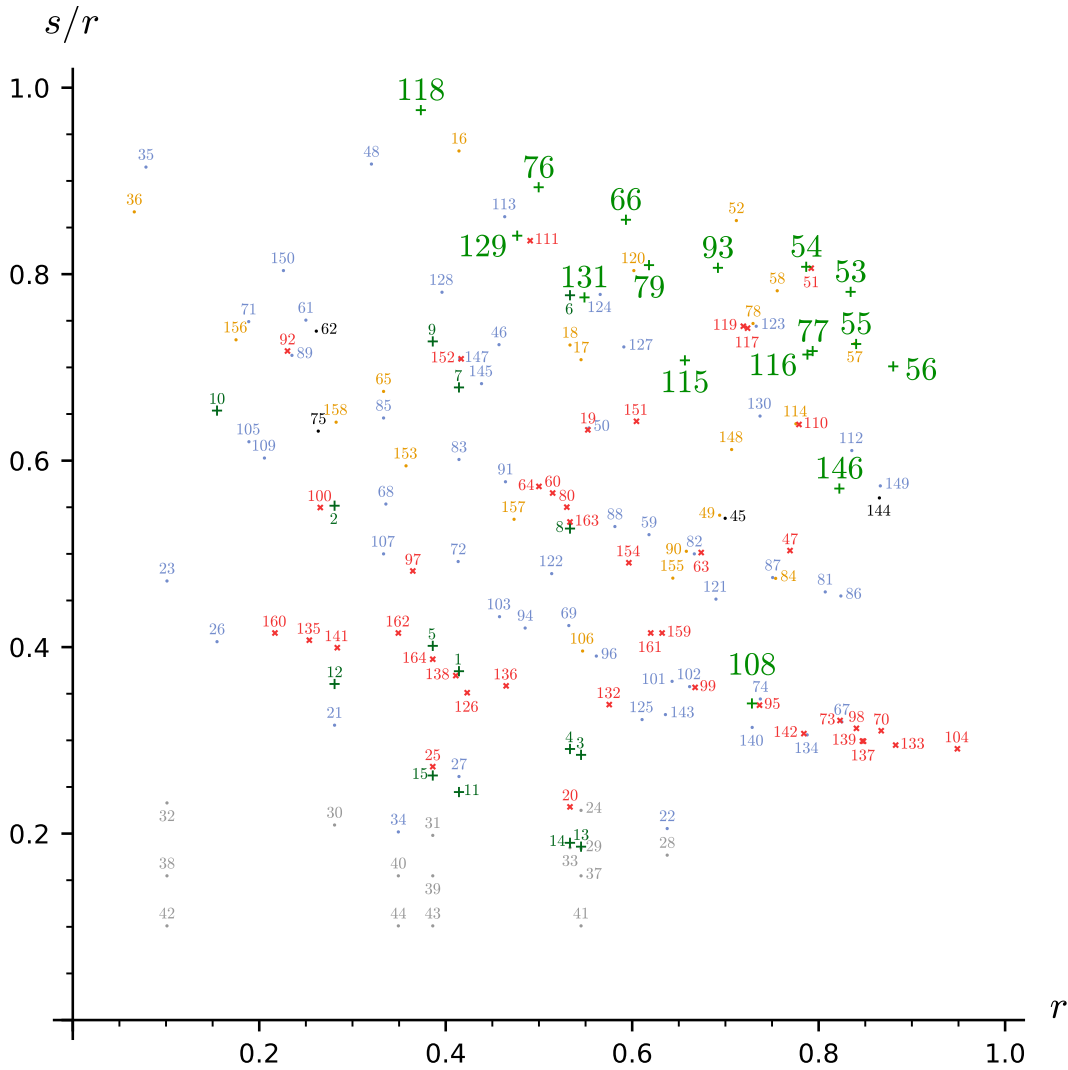
The values of radii corresponding to the cases from Theorem 4 are given in [15]. The triangulated packings maximizing the density for the cases from Th. 4.(a) are depicted in Fig. 5. For Th. 4.(b), the binary triangulated packings which maximize the density are present in Fig. 4 while the ternary triangulated packings are given in Fig. 7. An instance of a triangulated ternary packing and a non-triangulated binary denser packing for Th. 4.(c) are given in Fig. 8 while the complete list can be found in the appendix of the extended version of the paper [17].

All in all, we proved the Connelly conjecture to be false and classified the 149 cases where it was applicable in several groups: 16 cases for which the conjecture holds (Th. 4.(a)), 15 cases where the density is maximized on a triangulated packing using only two discs out of three (Th. 4.(b)), 40 (periodic) counter examples to the initial conjecture (Th. 4.(c)), and the other cases where our proof strategy does not work. Figure 6 represents each case (i.e. a triplet of disc radii $1, r, s$, $1 > r > s$) as a point with coordinates $(r, \frac{s}{r})$ and its number from [15]. The color of the point and the number corresponds to the class we assigned to the case.

Section 2 is dedicated to the cases where a ternary triangulated packing is proved to maximize the density. We explain the approach used in the similar proof for binary packings from [1] and how we enhance it to make it work in our context. The first improvement was the generalization of the code universal to all the cases (instead of treating them one by one as in [1]). The second necessary generalization was leaving a bunch of parameters as free variables instead of fixing them arbitrary. The theoretical background of the proof strategy is given in Section 2.1. Section 2.2 provides the main ideas of the computational part of the proof of Th. 4.(a) (the detailed version of this section is given in Section 3 of the full version [17]). We prove Th. 4.(b) in Section 2.3 by adjusting the proof of Th. 4.(a).



■ **Figure 5** The 16 triangulated ternary packings proved to maximize the density (the numbers correspond to the numbering in [15]).



■ **Figure 6** The “map” of the 164 cases with triangulated ternary packings. Each case (i.e. a triplet of disc radii $1, r, s, 1 > r > s$) corresponds to a point with coordinates $(r, \frac{s}{r})$ and its number from [15]. The cases where no triangulated packing is saturated are marked in grey. The cases with a ternary triangulated packing proved to maximize the density are marked by green + with larger case numbers. The cases where we proved a triangulated binary packing to maximize the density are marked by dark green +. The cases with counter examples are red (*). The cases featuring two coronas (find the details in Section 5.1) are orange. The cases with empty polyhedra (see Section 5.2) are blue. The remaining cases are marked in black (Section 5.3).

Our proof, as quite a few recent results in the domain, like [11,14,20], is based on computer calculations. The main details of the implementation are provided in Section 3. The complete code is given at the url: https://github.com/tooticki/ternary_triangulated_disc_packings.

Cases from Th. 4.(c) are treated in Section 4. We obtain a counter-example for each of these cases by applying the flip-and-flow method [3] on the triangulated binary packings with disc radii ratio close to the radii ratios of pairs of discs of this case.

Section 5 is dedicated to the remaining cases. Section 5.1 presents the 22 cases where one of the discs appears with at least two different neighborhoods. Our proof technique is not sufficient to treat such cases, handling them requires a less local approach.

Section 5.2 treats the 52 cases where we did not find a set of constants satisfying all required inequalities needed in our proof. Even though after several attempts with higher and higher precision, we concluded that the existence of valid constants is quite unlikely, it cannot be rigorously proved for the moment. We thus leave this as an open problem.

Finally, Section 5.3 is dedicated to the 4 cases where the existence of such set of constants is more probable since we could find the parameters satisfying the majority of constraints, but a few of them were still not satisfied. Whether the density is maximized in these cases is also an open problem.

2 Proof of Th. 4 (a) and (b)

In this section, we give the proof of the first two parts of Theorem 4. We follow almost the same steps of the proof as in [1] where the same result is proven for binary triangulated packings and in [13] which treats computationally the “simplest” case among the ternary triangulated packings (case 53).

From the theoretical point of view, the transition from binary packings to ternary ones seems to be straightforward. In practice, however, we have much more cases to treat (149 instead of 9) and for each of them, the problem is much more complex due to the high number of local combinatorial configurations in possible packings. This requires a more refined and sensitive choice of parameters than in [1].

2.1 Proof strategy

This section is strongly based on [1]: we use the idea of the proof and quite a few intermediate results. Thus, for the sake of simplicity, we preserve the same notations.

Let us describe the theoretical background of the proof which is common for all cases, the only difference being the choice of the parameters described in Section 3.

We are given 3 discs of radii $1, r$ and s , $1 > r > s$ and a ternary triangulated packing of the plane by copies of these discs conjectured to maximize the density, let us denote it by P^* . Our aim is to prove that for any other packing P using the same discs, its density $\delta(P)$ does not exceed the density δ^* of P^* .

The main idea common to all the results about the maximal density of triangulated packings was called “cell balancing” by Heppes [25] and it perfectly matches this title. It consists of two steps: first we locally “redistribute” the density among some well-defined cells (triangles of the triangulation in [1,25,27] and a mixture of Delaunay simplices and Voronoi cells, both encoded in so-called decomposition stars, in [23]) preserving the global density value. Then we prove that the redistributed density of any cell of P never exceeds δ^* .

First, let us define triangulations for packings by several sizes of discs. The *FM-triangulation* of a packing was introduced in [10] (it is a particular case of weighted Delaunay triangulations [5]). Some of its useful properties are given in [1] (Section 4). The vertices of

the FM-triangulation are the disc centers. There is an edge between two disc centers if and only if there is a point $p \in \mathbb{R}^2$ and a distance $d > 0$ such that p is at distance d from the both discs and at least d from any other disc.

Let \mathcal{T} and \mathcal{T}^* respectively denote the FM-triangulations of P and P^* . The cells we are interested in are the triangles of these triangulations. Instead of working with densities, we introduce an additive function E , called *emptiness*, which, for a triangle T in \mathcal{T} , is defined by

$$E(T) := \text{area}(T) \times \delta^* - \text{area}(T \cap P).$$

This function was used in [27] by the name of “excess”. It was inspired by “surplus area” introduced in [25] defined as $\text{area}(T) - \frac{\text{area}(T \cap P)}{\delta^*}$, identical to emptiness up to multiplication by δ^* . A similar but more complex function called “score” is used in the proof of the Kepler conjecture [29].

The emptiness function reflects how “empty” the triangle is compared to δ^* . Indeed, $E(T)$ is positive if the density of T is less than δ^* , negative if T is denser, and equals zero if $\delta(T) = \delta^*$. We use it rather than the density because of its additivity: the emptiness of a union of two triangles equals the sum of their emptiness values. This property does not hold for the density.

To prove that $\delta \leq \delta^*$, it is enough to show that $\sum_{T \in \mathcal{T}} E(T) \geq 0$ [1]. This intuitively means that P is globally more empty and less dense than P^* .

Instead of working directly with the emptiness, we define a so-called potential which plays the role of density redistribution mentioned above. We do it since this function, constructed explicitly, is easier to manipulate. We will construct a potential U such that for any triangle $T \in \mathcal{T}$, its potential does not exceed its emptiness:

$$E(T) \geq U(T) \tag{2}$$

and the sum of potentials of all triangles in \mathcal{T} is non-negative:

$$\sum_{T \in \mathcal{T}} U(T) \geq 0 \tag{3}$$

If, for P^* , there exists U satisfying (2) and (3) for any packing P , then P^* maximizes the density among packings using the same disc radii:

$$(2),(3) \implies \sum_{T \in \mathcal{T}} E(T) \geq 0 \implies \delta^* \geq \delta.$$

The rest of the proof consists in construction of potential U satisfying both (2) and (3) for any packing P .

2.2 Sketch of our proof of Th. 4 (a)

This section provides the short version of our proof, please find the detailed version in [17].

We follow the method of “localizing potentials” introduced by Kennedy in [27]. The idea is to distribute the potential U of each triangle among its vertices in a way that the sum of vertex potentials of the triangles around each vertex of any packing is non-negative. This local constraint of non-negativity implies inequality (3).

We choose the potential function as simple as possible to facilitate further calculations. As in [27] and [1], the potential in a vertex of a triangle depends only on the three disc radii of the triangle and the angle in the vertex.

Let us first introduce *tight triangles*: the triangles formed by three tangent discs. For ternary packings, there are always 10 of them. Let V_{xyz} denote the vertex potential of the tight triangle formed by discs of radii x, y, z in the vertex corresponding to the center of the y -disc, we call these constants *tight vertex potentials* and we fix them below.

Given a triangle T with discs of radii x, y, z and with vertex v in the center of the y -disc, we denote by \hat{v} the angle of v in T and by \widehat{xyz} the angle in the center of the y -disc of the tight triangle formed by the discs of radii x, y, z . We define the vertex potential of T in v as

$$\dot{U}_v(T) := V_{xyz} + m_y |\hat{v} - \widehat{xyz}|,$$

where m_y is a constant fixed below.

As in [1], we choose constants V_{xyz} and m_y in a way to satisfy the non-negativity around each vertex $v \in \mathcal{T}$:

$$\sum_{T \in \mathcal{T} | v \in T} \dot{U}_v(T) \geq 0. \tag{\bullet}$$

Besides that, tight vertex potentials should satisfy 5 equations in order to guarantee (2),(3) in P^* (you can find them in Section 3.2.1 of the full version of the paper [17]). In [1], the remaining tight vertex potentials are all set to 0 for the sake of simplicity. This strategy does not work in our case; we thus leave 6 tight vertex potentials $V_{1r1}, V_{1s1}, V_{r1r}, V_{rsr}, V_{s1s}, V_{srs}$ as free variables at this point.

The solutions of inequalities (\bullet) form a polyhedron in \mathbb{R}^9 containing all valid values of the tight vertex potentials and constants m_1, m_r, m_s . You can find more details on the vertex potentials in [17], the implementation details of the polyhedra are discussed in Section 3.2.

Choosing values of V_{xyz} and m_y among all the solutions found above, we seek to satisfy (2): we pick the solution where V_{xyz} and m_y are “small” (find details in [17]).

This is however not enough because of two “limit” cases of triangles. The first are so-called “stretched” triangles: those where one of the angles is very large which causes high vertex potential and low emptiness. However, the triangle sharing the longest edge of a stretched triangle always features low vertex potentials and high emptiness. We thus introduce an *edge* potential \bar{U} aiming to make stretched triangles share their potential with their empty neighbors. You can find the exact formulas of the edge potentials in Section 3.2.2 of the full version of the paper [17].

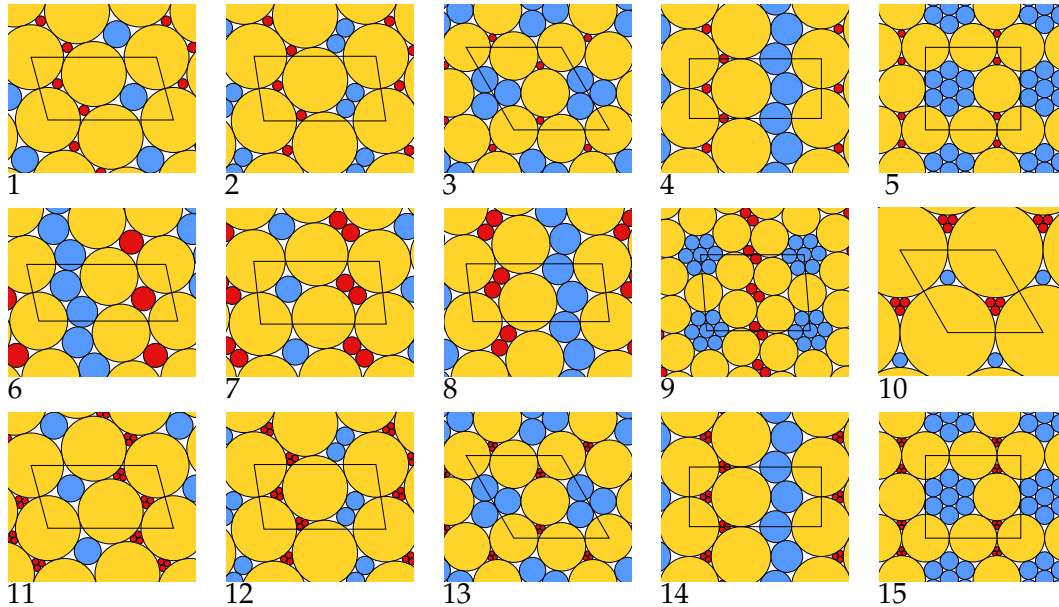
The second problematic case are so-called ϵ -tight triangles: those which are close to tight ones. In tight triangles, the emptiness is equal to the potential by definition which means that these values are close in ϵ -tight triangles. To verify (2) in this case, we have to compare the derivatives of the emptiness and the potential. This part is explained in Section 3.3.1 of [17].

As these cases are treated, we verify (2) for the remaining triangles using interval arithmetic which is discussed in Section 3.1. The details of this verification process are given in Section 3.3.2 of [17].

2.3 Proof of Th. 4 (b)

Cases 1-18 are special: they are called *large separated* in [15] since they do not contain pairs of adjacent medium and small discs (see Fig. 7 for the first 15). For each of these cases, in addition to ternary triangulated packings, there are other triangulated packings using only two discs out of three. It happens because the radii of small and medium discs coincide with the radii of small discs of two cases among b_1 – b_9 . It is thus possible to assemble

packings having the same density as the binary packings of mentioned cases using only two of three discs. It turns out that in all these cases, the density of one of the mentioned binary packings exceeds the density of the ternary one. That means, for each of cases 1-18, the densest packing among the triangulated ones is a binary packing corresponding to a case from b_1 - b_9 (Fig. 4).



■ **Figure 7** Triangulated ternary packings for cases 1-15, where a triangulated binary packing maximizes the density. For cases 1-5, it is the triangulated packing of b_8 ; for case 6 - b_4 ; for cases 7-9 - b_7 ; for cases 10-16 - b_9 .

Indeed, each of these ternary packings is formed as a “combination” of two binary packings one of which is denser than the other. Thus, the densest of the binary packings will also be denser than its combination with a less dense packing.

We were able to show that the denser triangulated binary packing maximizes the density among all packings (not only triangulated ones) for the cases from 1 to 15 (Fig. 7). The proof is almost the same as in Section 2.

Let i be the case number and P_3 denote its triangulated ternary packing. Let P_2^* denote the densest triangulated binary packing using two discs of case i and let P_2 denote the less dense triangulated binary packing using two discs of case i . We already know that P_2^* is denser than the two others, $\delta(P_2^*) > \delta(P_3) > \delta(P_2)$. Our aim is to show that P_2^* maximizes the density among all packings by the discs of case i .

The only difference with the strategy used for other cases concerns vertex potentials. Since P_2^* uses only two discs out of three, it features only 2 coronas instead of 3. Thus, these 2 coronas together with the 10 equations for tight triangles, give us at most 11 independent equations instead of 12.

We now need to chose 7 free variables instead of 6. We can pick 6 tight potentials of isosceles triangles as before. There remains to choose the last free variable. Vertex potentials of equilateral tight triangles cannot be picked because of the equations of type $V_{xxx} = E_{xxx}$: they are already fixed. The remaining vertex potentials of isosceles triangles (V_{xxy} , $x \neq y$) cannot be used since they are dependent of the first 6 free variables and the equations $2V_{xxy} + V_{xyx} = E_{xyx}$. The only candidates thus are $V_{1rs}, V_{1sr}, V_{r1s}$; we add one of them.

32:12 When Ternary Triangulated Disc Packings Are Densest

For cases 16, 17, and 18, the densest binary packing is b_5 which features two different coronas around the small disc, so our method is not applicable to them as discussed in Section 5.1.

To summarize, for cases 1-18, among triangulated packings, the density is maximized by a binary packing, not a ternary one as in the Connelly conjecture. However, whether this packing maximizes the density among all packings is still an open question for cases 16–18.

3 Computer implementation

As many proofs of the domain, notably the proof of the Kepler Conjecture [20], the proofs of the maximal density for triangulated packings, like ours and those from [1, 13, 27], essentially rely on computer calculations. In this section, we discuss the details of computer implementation. You can find the complete code at https://github.com/tooticki/ternary_triangulated_disc_packings.

The treatment of each case consists of two steps summarized in Section 2.2. We first choose all the values necessary to define the potential: tight vertex potentials V_{xqy} , constants m_q and capping values Z_q (Section 3.2.1, [17]), the value of ϵ (Section 3.3.1, [17]), and the constants l_{xy}, q_{xy} of the edge potentials (Section 3.2.2, [17]). We choose them in a way to satisfy the “global” inequality (3). The second step is to verify the “local” inequality (2) on all possible triangles.

3.1 Interval arithmetic

We use interval arithmetic in two completely different contexts: to work with real numbers non representable in computer memory and to verify inequalities on uncountable but compact sets of values. More precisely, we use intervals to store the values of radii of discs which are algebraic numbers obtained as roots of polynomials in [15] as well as the value of π . The other situation where we use intervals is to verify the local inequalities on a compact continuum set of triangles.

In interval arithmetic, each value is represented by an interval which contains it and whose endpoints are exact values finitely representable in computer memory (floating-point numbers). Performing functions in interval arithmetic preserves both properties. More precisely, if x_1, \dots, x_n are intervals, and f is an n -ary function, the interval $f(x_1, \dots, x_n)$ must contain $f(y_1, \dots, y_n)$ for all $(y_1, \dots, y_n) \in x_1 \times \dots \times x_n$ and its endpoints are floating-point numbers.

To verify an inequality on two intervals $x_1 < x_2$, it is enough to compare the right endpoint of x_1 and the left endpoint of x_2 . The returned value is `True` only if each pair of values from these intervals satisfy the inequality. However, if the result is `False`, that does not mean that the inequality is false on the numbers represented by x_1 and x_2 , it might also mean that these intervals overlap.

We worked with interval arithmetic implemented in SageMath [6], called Arbitrary Precision Real Intervals¹. The intervals endpoints are floating-point numbers, the precision we use in the majority of cases is the default precision of the library where the mantissa encoding has 53 bits.

¹ https://doc.sagemath.org/html/en/reference/rings_numerical/sage/rings/real_mphi.html

3.2 Polyhedra

As mentioned in Section 2.2, we choose the values of vertex potentials in tight triangles and constants m_1, m_r, m_s in a way to satisfy all the necessary constraints (more details are given in [17]). These constraints together define a subset of \mathbb{R}^9 (where the variables are 6 tight vertex potentials $V_{1r1}, V_{1s1}, V_{r1r}, V_{rsr}, V_{s1s}, V_{sr s}$ and 3 constants m_1, m_r, m_s). We use the Polyhedra module² of SageMath to work with them (it allows us to store the solutions of a system of linear inequalities as a convex polyhedron).

Even more constraints are added by ϵ -tight triangles, since there should exist a positive value of ϵ satisfying the inequalities on derivatives of emptiness and potential given in [17]. To guarantee that, we verify if the inequality hold for $\epsilon = 0$, in other words, we make sure that it holds for some non-negative ϵ . We do it in SageMath: to compute both parts of the inequality, we use interval arithmetic and calculations of derivatives. The obtained inequalities are intersected with the polyhedron calculated above. For all the cases considered in this section, this intersection is not empty (the cases where it was empty are discussed in Section 5.2). Then we find the maximal value of $\epsilon > 0$ allowing the intersection not to be empty and this permits us to fix ϵ .

For all the cases treated in this section, these constraints together define a compact polyhedron in \mathbb{R}^9 (where the variables are the 6 tight vertex potentials and m_1, m_r, m_s).

After we get a polyhedron of valid values, we are free to choose a point inside to fix them. Our aim at that step is to minimize potentials of all triangles in order to satisfy (2). We thus find the three vertices of the polyhedron minimizing m_1, m_r and m_s respectively, compute a linear combination of them (the weights that worked well in practice were respectively 1,1 and 4), and take a point between this one and the center of the polyhedron in order to avoid the approximations problems on the border which are discussed in the next paragraph. Our method to choose the point described above is a heuristic.

Implementing construction of polyhedra, we encounter the following problem: the Polyhedra class does not allow coefficients of constraints to be intervals, while some of the coefficients of our inequalities are stored as such due to their dependency of π and disc radii. Polyhedra do not support intervals as a base ring for a good reason: solutions of a system of linear inequalities with interval coefficients might not form a convex polyhedron. We choose to replace the intervals with their centers and work with an approximation of the actual set of valid values for tight potentials and m_1, m_r, m_s . Our polyhedron is stored in a field of rational values, since this field is computationally quite efficient.

That means, after choosing a point inside this approximated polyhedra, we cannot know if this point actually satisfies all the constraints. To make sure it does, we then rigorously verify that all the inequalities with interval coefficients hold in this point.

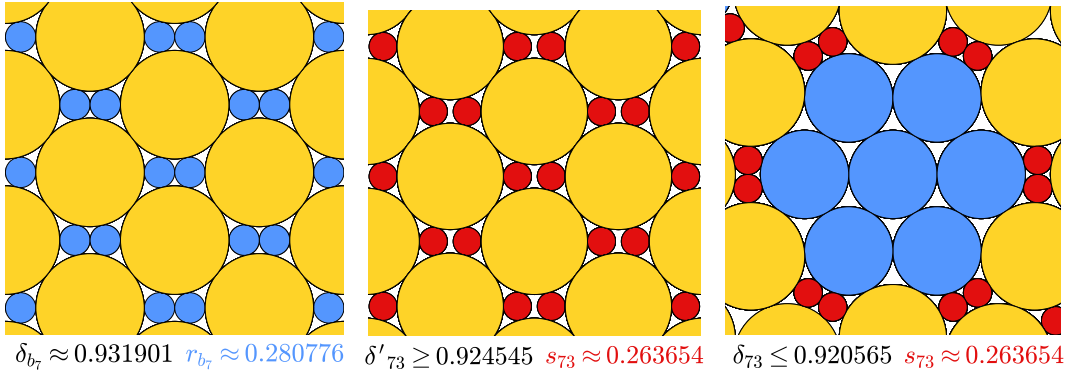
4 Counter-examples: proof of Th. 4 (c)

Starting to work on the density of ternary saturated triangulated packings, we believed the Connelly conjecture to hold, i.e. that for all of the 149 cases, a triangulated packing would maximize the density. Realization that our proof strategy failed for many of them made us suspect the conjecture to be false. Knowing that the density of binary triangulated packings (all of them are given in Figure 4) often exceeds the density of ternary triangulated packings in question gave us an idea to use them in order to find counter examples.

² https://doc.sagemath.org/html/en/reference/discrete_geometry/sage/geometry/polyhedron/constructor.html

32:14 When Ternary Triangulated Disc Packings Are Densest

The first result we obtained was for case 110 [16]. After generalization, we ended up with 40 counter examples (19, 20, 25, 47, 51, 60, 63, 64, 70, 73, 80, 92, 95, 97, 98, 99, 100, 104, 110, 111, 117, 119, 126, 132, 133, 135, 136, 137, 138, 139, 141, 142, 151, 152, 154, 159, 161, 162, 163, 164). They are all non triangulated packings using only two discs out of three which have greater densities than triangulated packings using all three discs. We obtained each of them deforming a triangulated binary packing with discs whose size ratio is close to the one of a pair of discs in the triplet associated to the case. Tiny deformations do not dramatically lower the density and these packings are dense enough to beat the ternary triangulated ones.



■ **Figure 8** Left: a triangulated binary packing of case b_7 . Middle: a deformation where the small discs are replaced with the small discs of case 73. Right: a triangulated periodic packing of case 73, its fundamental domain and description are given in [15].

Let us explain our method on an example. Recall that the pairs of discs allowing binary triangulated packings are denoted by b_1, \dots, b_9 while the triplets with ternary triangulated packings are indexed by positive integers from 1 to 164. Let us consider case 73, its triangulated ternary packing is given in Figure 8, on the right. Notice that the radius of the small disc ($s_{73} \approx 0.263$) of case 73 is close to the radius of the small disc ($r_{b_7} \approx 0.281$) of case b_7 . Let us deform the triangulated binary packing of b_7 (Figure 8, on the left) replacing the small disc of b_7 by the small disc from 73. We choose a deformation which breaks as few contacts between discs as possible (Figure 8, in the middle). Observe that the only broken contact is between the two small discs: they are not tangent anymore. The density of this new non-triangulated packing $\delta' \approx 0.9245$ is higher than the density of the triangulated packing 73 $\delta_{73} \approx 0.9206$ (Figure 8, on the right).

This method is called flip-and-flow [3]. The 40 counter examples were found by computer search. First, for each case b_i , we find the set of pairs of radii from the cases 1-164 with radii ratio “close enough” (we choose the distance heuristically) to the ratio of the discs of b_i . Then we deform the triangulated packing of b_i to obtain packings with the found disc ratios. Our way to deform packings was chosen in order to minimize the number of broken contacts between discs since intuitively it is the best way to keep the density high. Finally, the densities of 40 packings obtained by our method were higher than the densities of the respective ternary triangulated packings which leaves us with the counter examples illustrated in the appendix of the full version of the paper [17].

Our method is not universal: there might be other deformations for certain cases to obtain even higher density and even more counter examples. Besides that, there might be other cases with ternary counter examples (notably, among the cases discussed in Sections 5.2).

5 Other cases

5.1 2 coronas

Among the necessary conditions on vertex potentials in tight triangles given in [17], we saw that the sum of potentials in the corona around any vertex of triangulated packing T^* must be equal to zero. In all the proved cases, each disc has only one possible corona in T^* . It is not always the case, more precisely, among the cases where T^* is saturated, and for which we did not find counter examples, there are 22 cases where one of the discs appears with at least two different coronas in T^* : 16, 17, 18, 36, 49, 52, 57, 58, 65, 78, 84, 90, 106, 114, 120, 148, 153, 155, 156, 157, 158, 160. Each of these cases features a supplementary corona consisting of 6 discs of the same size as the central one. We thus have to add a supplementary condition $6V_{xxx} = 0$, where x is the radius of the disc with two coronas. This however contradicts the condition $3V_{xxx} = E_{xxx}$ in all of these cases. Our density redistribution would need to be less local to solve this problem. In the context of binary triangulated packings, such a case (b_5 , see Figure 4) is treated in detail in Section 5.3 of [1].

5.2 Empty polyhedra

In Section 3.2, we construct a polyhedron in \mathbb{R}^9 aiming to contain all valid values of tight vertex potentials and m_1, m_r, m_s . In this section, we talk about the 52 cases where the polyhedron obtained by our computations is empty: 21, 22, 23, 26, 27, 34, 35, 46, 48, 50, 59, 61, 67, 68, 69, 71, 72, 74, 81, 82, 83, 85, 86, 87, 88, 89, 91, 94, 96, 101, 102, 103, 105, 107, 109, 112, 113, 121, 122, 123, 124, 125, 127, 128, 130, 134, 140, 143, 145, 147, 149, 150.

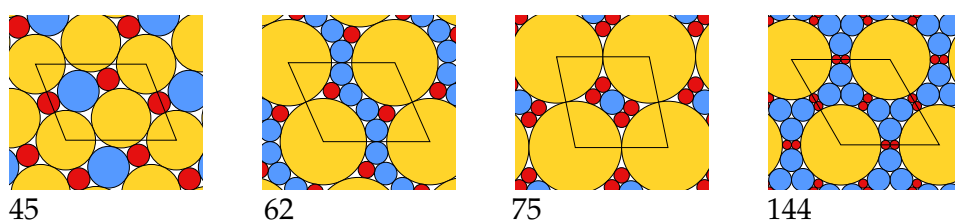
The polyhedron formed by the inequalities on vertex potentials and the inequality for ϵ -triangles (which are given in [17]), represents the values satisfying (\bullet) featuring a non-negative valid ϵ . These constraints are necessary for our proof to be correct. If this polyhedron is empty there are no valid values of tight potentials and m_1, m_r, m_s and thus our strategy of proof is not applicable.

Nevertheless, our computations are limited by computer memory which can represent only certain values. Normally, we avoid this problem by using interval arithmetic (Section 3.1). However, we can not apply this solution with polyhedra. First, as mentioned in Section 3.2, in SageMath, the polyhedra module does not support the interval field as a base ring. Implementing another way to represent “interval polyhedra” would be unreasonable due to memory and time constraints of calculations: the polyhedra are constructed from thousands of inequalities, and performing computations in interval field significantly increases time and memory costs. Instead, we use the ring of rationals to store the inequalities coefficients. Therefore, the polyhedron we work with is an approximation of the actual polyhedron and may not contain all the valid sets of values.

Yet, we believe that the polyhedra in question are probably actually empty in these cases, so the precision issues are not the principal obstacle. All in all, some of the cases from this section might actually maximize the density but we would need an essentially different approach to be able to prove it. Looking forward, further attempts to treat these cases would likely need to use a less local density distribution.

5.3 The 4 mysterious cases

In the four remaining cases (45, 62, 75, and 144) the polyhedron from Section 3.2 is not empty, like for the cases from the previous section. Nevertheless, we could not find a point in it to guarantee the local inequality (2) in all triangles: the problematic triangles are always



■ **Figure 9** Triangulated ternary packings of the four *mysterious* cases.

those close to one of the tight ones. Minimizing m_q and the tight potentials is an obvious strategy to minimize the potentials and eventually satisfy (2) but the capping constants Z_q also dramatically affect potentials.

Trying to find appropriate values of V_{xyz} , m_q and Z_q , we represented all the constraints coming from (3) as a linear optimization problem. This allowed us to encode problematic triangles violating (2) as constraints and add them to the system, one by one, each time one appears during local verification, in hope to finally “converge” to a solution which would satisfy (2) on all triangles. However, this method failed: no solutions were found.

The fact that we could not choose a set of appropriate constants in these cases does not prove that they do not exist (due to the approximation issues already discussed in the previous section as well as the new ones coming from encoding our constraints into a rational linear problem). We, however, believe that these cases, as well as those from the previous section, just cannot be treated by our proof methods. They probably require a less local emptiness redistribution than the one we use.

References

- 1 N. Bedaride and T. Fernique. Density of Binary Disc Packings: The Nine Compact Packings. *Discrete and Computational Geometry*, 67:1–24, 2022. doi:10.1007/s00454-021-00348-7.
- 2 R. Connelly, S. Gortler, E. Solomonides, and M. Yampolskaya. Circle packings, triangulations, and rigidity. *Oral presentation at the conference for the 60th birthday of Thomas C. Hales*, 2018.
- 3 R. Connelly and S. J. Gortler. Packing Disks by Flipping and Flowing. *Discret. Comput. Geom.*, 66:1262–1285, 2021.
- 4 J. Conway and N.J.A. Sloane. *Sphere Packings, Lattices and Groups*. Grundlehren der mathematischen Wissenschaften. Springer New York, 1998.
- 5 S. L. Devados and J. O’Rourke. *Discrete and Computational Geometry*. Princeton University Press, 2011.
- 6 The Sage Developers. Sage mathematics software (version 9.0). <http://www.sagemath.org>, 2020.
- 7 E. Fayen, A. Jagannathan, G. Foffi, and F. Smallenburg. Infinite-pressure phase diagram of binary mixtures of (non)additive hard disks. *The Journal of Chemical Physics*, 152(20):204901, 2020.
- 8 L. Fejes Tóth. Über die dichteste Kugellagerung. *Math. Z.*, 48:676–684, 1943. doi:10.1007/BF01180035.
- 9 L. Fejes Tóth. Compact Packing of Circles. *Studia Sci. Math. Hungar.*, 19:103–107, 1984.
- 10 L. Fejes Tóth and J. Molnár. Unterdeckung und Überdeckung der Ebene durch Kreise. *Mathematische Nachrichten*, 18:235–243, 1958.
- 11 S. P. Fekete, P Keldenich, and C. Scheffer. Packing disks into disks with optimal worst-case density. *Discrete and Computational Geometry*, 2022. doi:<https://link.springer.com/article/10.1007/s00454-022-00422-8>.

- 12 S. P. Fekete, S. Morr, and C. Scheffer. Split packing: Packing circles into triangles with optimal worst-case density. In *Algorithms and Data Structures*, pages 373–384. Springer International Publishing, 2017.
- 13 T. Fernique. A densest ternary circle packing in the plane. <https://arxiv.org/abs/1912.02297>, 2019.
- 14 T. Fernique. Density of binary disc packings: Lower and upper bounds. *Experimental Mathematics*, pages 1–12, 2022.
- 15 T. Fernique, A. Hashemi, and O. Sizova. Compact packings of the plane with three sizes of discs. *Discret. Comput. Geom.*, 66(2):613–635, 2021.
- 16 T. Fernique and D. Pchelina. Compact packings are not always the densest. <https://arxiv.org/abs/2104.12458>, 2021.
- 17 T. Fernique and D. Pchelina. Density of triangulated ternary disc packings. <https://arxiv.org/abs/2211.02905>, 2022.
- 18 A. Florian. Ausfüllung der Ebene durch Kreise. *Rendiconti del Circolo Matematico di Palermo*, 9:300–312, 1960.
- 19 C. F. Gauss. Untersuchungen über die Eigenschaften der positiven ternären quadratischen Formen von Ludwig August Seber. *Göttingische gelehrte Anzeigen*, 1831.
- 20 T. C. Hales. A proof of the Kepler conjecture. *Annals of Mathematics*, 162(3):1065–1185, 2005.
- 21 T. C. Hales, M. Adams, G. Bauer, D. T. Dang, J. Harrison, T. L. Hoang, C. Kaliszyk, V. Magron, S. McLaughlin, T. T. Nguyen, T. Q. Nguyen, T. Nipkow, S. Obua, J. Pleso, J. Rute, A. Solovyev, A. H. T. Ta, T. N. Tran, D. T. Trieu, J. Urban, K. K. Vu, and R. Zumkeller. A formal proof of the Kepler conjecture. *Forum of Mathematics, Pi*, 5:e2, 2017. doi:10.1017/fmp.2017.1.
- 22 T. C. Hales and S. P. Ferguson. The Kepler conjecture. *Discrete Comput. Geom.*, 36(1):1–269, 2006.
- 23 T. C. Hales and S. P. Ferguson. *A Formulation of the Kepler Conjecture*, pages 83–133. Springer New York, New York, NY, 2011.
- 24 A. Heppes. On the densest packing of discs of radius 1 and $\sqrt{2} - 1$. *Studia Scientiarum Mathematicarum Hungarica*, 36:433–454, 2000.
- 25 A. Heppes. Some densest two-size disc packings in the plane. *Discrete and Computational Geometry*, 30:241–262, 2003.
- 26 A. B. Hopkins, F. H. Stillinger, and S. Torquato. Densest binary sphere packings. *Phys. Rev. E*, 85:021130, 2012.
- 27 T. Kennedy. A densest compact planar packing with two sizes of discs. <https://arxiv.org/abs/math/0412418>, 2005.
- 28 T. Kennedy. Compact packings of the plane with two sizes of discs. *Discret. Comput. Geom.*, 35(2):255–267, 2006. doi:10.1007/s00454-005-1172-4.
- 29 J. Lagarias. Bounds for local density of sphere packings and the Kepler conjecture. *Discrete and Computational Geometry*, 27:165–193, 2002. doi:10.1007/s00454-001-0060-9.
- 30 M. Messerschmidt. The number of configurations of radii that can occur in compact packings of the plane with discs of n sizes is finite. <https://arxiv.org/abs/2110.15831>, 2021. doi:10.48550/ARXIV.2110.15831.
- 31 P. I. O’Toole and T. S. Hudson. New high-density packings of similarly sized binary spheres. *The Journal of Physical Chemistry C*, 115(39):19037–19040, 2011.
- 32 T. Paik, B. T. Diroll, C. R. Kagan, and C. B. Murray. Binary and Ternary Superlattices Self-Assembled from Colloidal Nanodisks and Nanorods. *Journal of the American Chemical Society*, 137(20):6662–6669, 2015.
- 33 A. Thue. Über die dichteste Zusammenstellung von kongruenten Kreisen in einer Ebene. *Christiania Videnskabs-Selskabets Skrifter*, I. Math.-Naturv. Klasse, 1:1–9, 1910.